Biochemical Pharmacology, Vol. 42, No. 2, pp. 337–346, 1991.
Printed in Great Britain.

0006-2952/91 $3.00 + 0.00

METABOLISM OF A NOVEL ANTITUMOR AGENT, CRISNATOL, BY A HUMAN HEPATOMA CELL LINE, Hep G2, AND HEPATIC MICROSOMES

CHARACTERIZATION OF METABOLITES

DIPAK K. PATEL,* JOHN P. SHOCKCOR, SAI Y. CHANG, CARL W. SIGEL and BRIAN E. HUBER

Burroughs Wellcome Co., Research Triangle Park, NC 27709, U.S.A.

(*Received* 24 *October* 1990; *accepted* 8 *February* 1991)

Abstract—Metabolism of the anticancer agent crisnatol was investigated using a human hepatoma cell line, Hep G2, and human liver microsomes. Crisnatol was metabolized extensively by both systems. The TLC/autoradiographic analysis showed that the crisnatol metabolite profile was similar for both systems and the major metabolites were shown to have structural characteristics similar to those formed by the rat. The Hep G2 cells formed three isomeric dihydrodiols; one of these has been identified by GC/MS and ^{1}H-NMR as the crisnatol 1,2-dihydrodiol. Human liver microsomes also formed two isomeric dihydrodiols with 1,2-dihydrodiol as the major isomer and, in addition, produced 1-hydroxycrisnatol. Crisnatol concentrations of 1.3 μg/mL completely inhibited the replication of Hep G2 cells as measured by thymidine incorporation and cell growth kinetics and, at this concentration, cell viability decreased by only 35% as determined by vital staining of cells using neutral red dye.

Crisnatol, 2-[(6-chrysenylmethyl)amino]-2-methyl-1,3-propanediol (BW A770U), is a member of a series of novel DNA intercalating arylmethylaminopropanediol (AMAP†) antitumor agents [1]. This lipophilic compound has displayed significant antitumor activity in murine and human tumor models [2–4] and is currently undergoing phase II clinical trials. Preclinical metabolism and disposition of crisnatol in animals have been investigated extensively [5–7], but its mechanism of action and biotransformation in humans still remain to be determined. Preliminary pharmacokinetic data from phase I clinical trials suggest rapid hepatic clearance of crisnatol presumably due to metabolism and/or biliary excretion but specific crisnatol metabolites have not been identified [8]. Metabolism studies including isolation and characterization of metabolites form an integral part of preclinical drug development and the information derived from these studies may contribute significantly to elucidating the mechanisms of action and toxicity of new therapeutic agents.

Several recent reports suggest that human hepatoma cell lines may serve as a useful *in vitro* model system for studying carcinogen activation and drug metabolism. One such cell line, Hep G2, established from a human hepatoblastoma [9], has been shown to retain many of the specialized functions of normal liver parenchymal cells including expression of hepatocyte-specific cell surface receptors [10–12], and synthesis and secretion of plasma proteins [13–15]. Hep G2 cells also retain drug-metabolizing capacity, both the cytochrome P450-dependent mixed-function oxidases as well as glucuronic acid and sulfate-conjugating activities [16–19]. These cells metabolically activate cyclophosphamide, benzo[*a*]pyrene, aflatoxin B_1, diethylstilbestrol and benzidine into mutagenic and cytotoxic products [20–24]. In addition, Hep G2 cells metabolize endogenous compounds such as cholesterol and other lipoproteins [25–27].

The specific objectives of the present study were to compare the metabolic pathways of crisnatol in Hep G2 cells and normal human liver microsomes, and to isolate and characterize major metabolites. In addition, we assessed the antiproliferative activity of various concentrations of crisnatol in Hep G2 cells by measuring thymidine incorporation, cell growth, and vital staining of cells using neutral red dye.

MATERIALS AND METHODS

Materials. All compounds used were of analytical grade. [^{14}C]Crisnatol mesylate, 2-[(6-chrysen[5,11-^{14}C]yl-methyl)amino]-2-methyl-1,3-propanediol methanesulfonate (mesylate), was synthesized by Dr. J. Hill at the Wellcome Research Laboratories (Research Triangle Park, NC) with a specific activity of 48.50 mCi/mmol and a radiochemical purity of greater than 97%. Thymidine[*methyl*-^{3}H], with a specific activity of 25 Ci/mmol, was purchased from the Amersham Corp. (Arlington Heights, IL). D-Glucose-6-phosphate, NADPH, D-saccharic acid

* Send reprint requests to: Dr. Dipak K. Patel, Division of Medicinal Biochemistry, Wellcome Research Laboratories, 3030 Cornwallis Road, Research Triangle Park, NC 27709.

† Abbreviations: AMAP, arylmethylaminopropanediol; DMSO, dimethyl sulfoxide; TCA, trichloroacetic acid; PBS, phosphate-buffered saline; TMS, trimethylsilyl; BSTFA, *N,O*-bis-(trimethylsilyl)trifluoroacetamide; EI/MS, electron-impact/mass spectra; GC/MS, gas chromatography/mass spectrometry; and ^{1}H-NMR, proton nuclear magnetic resonance.

1,4-lactone (inhibitor for β-glucuronidase), glucose-6-phosphate dehydrogenase (Type IX), and a β-glucuronidase/sulfatase mixture (*Helix pomatia*; type VII) were obtained from the Sigma Chemical Co. (St. Louis, MO). Bond Elut (3 cc, C_{18}) cartridges were obtained from Analytichem International (Harbor City, CA) and Sep Pak (C_{18}) from Waters Chromatography Division (Milford, MA). Chromatographic solvents were HPLC grade.

Cell culture and antiproliferation assays. Hep G2 cells were cultured as previously described [28]. For cell culture experiments, crisnatol was dissolved in DMSO and at all times the final DMSO concentration in the cell culture medium was below 0.16%.

[^{3}H]Thymidine incorporation into DNA was determined in Hep G2 cells growing in the absence and presence of various concentrations of crisnatol. Cells were plated at a density of 2×10^5 cells/2 mL medium/well in a 12-well plate. After the indicated periods of time in the presence of crisnatol, 10 μCi [^{3}H]thymidine were added for a 45-min pulse; then radioactivity was determined in acid-insoluble and acid-soluble pools by TCA precipitation and liquid scintillation counting as previously described [29]. Preliminary studies showed that radioactivity was linearly incorporated into acid-insoluble pools for at least 3 hr. Staining with the vital stain, neutral red, was performed by plating either 3000 or 6000 cells/0.1 mL medium/well in a 96-well microtiter dish on day −1. On day 0, various concentrations of crisnatol were added in a 100 μL volume and, at the indicated periods of time, neutral red staining was determined as previously described [30].

Crisnatol metabolism by Hep G2 cells. Metabolism of [^{14}C]crisnatol by Hep G2 cells was determined at 0.05, 0.50 and 1.00 μg crisnatol/mL culture medium. Cells were plated at 1×10^6 cells/25 cm^2/5 mL culture medium on day −1, [^{14}C]crisnatol was added on day 0 and the incubation continued for an additional 24 hr. In other studies, cells were incubated with 1.00 μg [^{14}C]crisnatol/mL culture medium for 0.5, 1.0, 3.0, 5.5, and 24 hr. At the end of each incubation period, the medium was removed and the cells were washed with 5 mL PBS; then 10 mL of a methanol/water mixture (75:25, v/v) was added. The cells were lysed by sonication and then centrifuged at 3000 rpm for 15 min to obtain a supernatant, which was designated as "intracellular supernatant." Culture flasks were rinsed with scintillation fluid to determine the residual radioactivity. The cell culture medium (1 mL) was applied to a 3 cc Bond Elut (C_{18}) solid-phase disposable cartridge which was preconditioned by washing with methanol (3 mL) followed by water (6 mL). The cartridges were washed with water (9 mL) and radioactive material was eluted by washing with methanol (3 mL) which was subsequently reduced to dryness. The residues were redissolved in methanol and then assayed for crisnatol and metabolites by TLC/autoradiography (see below).

The above procedure was scaled-up using 2.5×10^7 cells/150 cm^2/25 mL of cell culture medium containing 1.0 μg [^{14}C]crisnatol/mL to generate crisnatol metabolites for structural characterization.

Crisnatol metabolism by human liver microsomes. Human liver microsomes were obtained as described previously [31]. The incubation mixture consisted of 2 mL of 0.2 M potassium phosphate buffer (pH 7.4), 5 mM $MgCl_2$, 7.5 mM glucose-6-phosphate, 1.75 mM NADPH, 1 unit glucose-6-phosphate dehydrogenase and human liver microsomes (11.23 mg protein) in a 5-mL final incubation volume. The reaction was initiated by adding [^{14}C]crisnatol at the indicated concentrations, and then the mixture was incubated at 37° with constant shaking. After 24 hr, the reaction was stopped by adding an equal volume of methanol/acetonitrile (1:1). The resultant mixture was then centrifuged at 3000 rpm for 15 min and the supernatant assayed by TLC/autoradiography (see below). The above procedure was repeated on a larger scale in the presence of both the non-labeled (1 mg) and [^{14}C]crisnatol to generate crisnatol metabolites for structural characterization.

TLC/autoradiography. Analytical TLC was performed on glass plates (20 × 20 cm) precoated with 0.25 mm silica gel 60 (E. Merck, Darmstadt, West Germany). The developing solvent system was dichloromethane/methanol/ammonium hydroxide/water (65:30:1:3, by vol.). The TLC plates were developed for 14 cm and radioactive bands located by autoradiography using X-ray film (Kodak SB 5, Rochester, NY). The distribution of radioactivity applied on the plate was determined by scraping discrete sections of the silica gel into scintillation vials followed by liquid scintillation counting.

Radioactivity measurement. Samples (50 μL) were assayed in replicate for radioactivity in a Packard Tri-Carb, model 460 CD liquid scintillation counter (Packard Instruments, Downers Grove, IL) using 10 mL of Aquasol-2 (Packard) scintillation fluid. For samples containing cellular extracts, cell debris was first solubilized using Soluene-100 (Packard) tissue solubilizer.

Isolation of crisnatol metabolites. Crisnatol metabolites formed by Hep G2 cells were isolated as follows: Pooled cell medium was applied to an Amberlite XAD-2 resin column followed by a water wash. The column was then sequentially washed with ethyl acetate/acetone (1:1), methanol, and methanol/triethylamine (8:2) to elute the majority of the ^{14}C-labeled material. The organic fractions were combined and their volume was reduced to dryness. The residue was redissolved in water and then applied to a Sep Pak (C_{18}) cartridge which was washed with water and then eluted with methanol/triethylamine (8:2). The methanol/triethylamine eluent was reduced to dryness and the resultant residue redissolved in methanol and chromatographed on preparative silica gel TLC plates as described above. Autoradiograms of the developed plates revealed three major bands at R_f values of 0.61 (band A), 0.65 (band B) and 0.69 (band C). The silica gel corresponding to band A, and bands B + C combined (since these bands ran very close together) was removed and the radioactivity was eluted from silica gel with methanol, which was reduced to dryness. The two compounds obtained from bands B and C were further purified by HPLC. The HPLC system consisted of a Waters 600 multisolvent delivery pump, a Waters WISP 712 autoinjector, and a Kratos variable wavelength UV detector (Spectroflow 757). Crisnatol metabolites

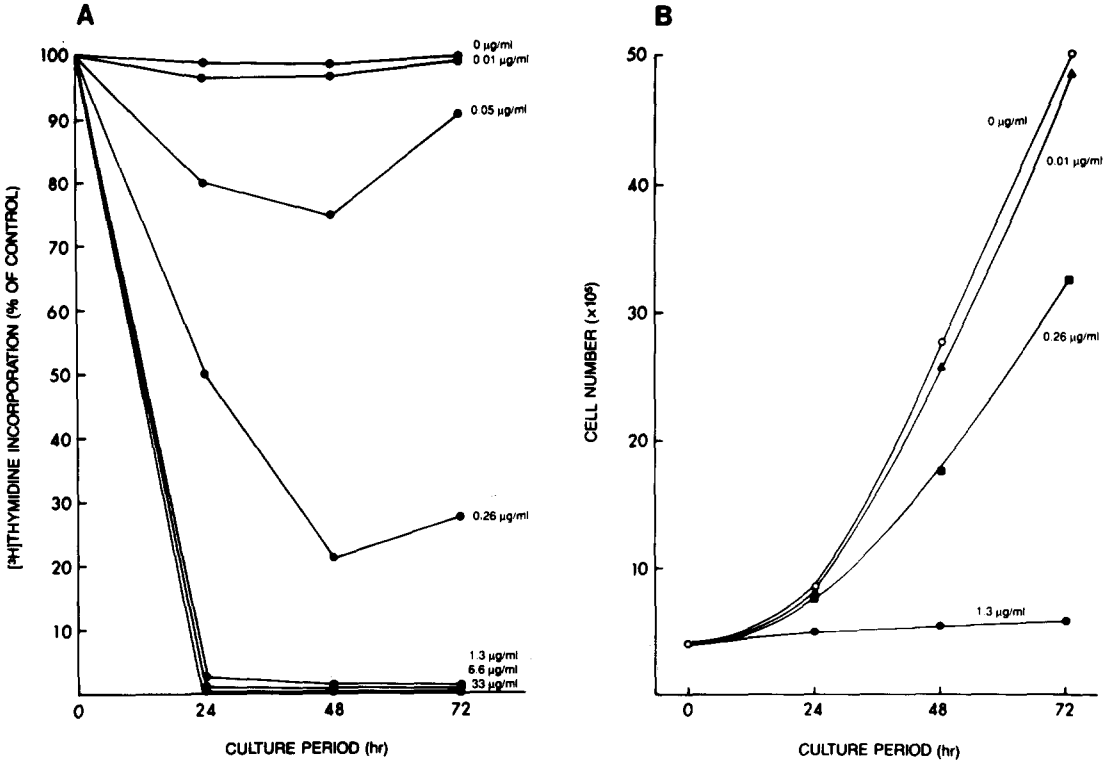

Fig. 1. (A) [^{3}H]Thymidine incorporation into acid-insoluble pools of Hep G2 cells cultured with various concentrations of crisnatol. Cells were cultured in the presence of the indicated concentrations of crisnatol for 24, 48 and 72 hr. Radioactivity was determined in acid-insoluble pools. Data are expressed as a percentage of controls which received no treatment. Values for total radioactivity incorporated into the control samples at 24, 48 and 72 hr were 2.2×10^5, 2.5×10^5 and 2.8×10^5 dpm, respectively. The 0 μg/mL values represents vehicle-treated samples. Each point represents three independent determinations. (B) Growth rate of Hep G2 cells cultured with various concentrations of crisnatol for 24, 48 and 72 hr. Hep G2 cells were plated on day −1. On day 0 crisnatol was added at the indicated concentrations. Cell number determinations were made on day 0 and after 24, 48 and 72 hr. The line labeled 0 μg/mL represents vehicle-treated control cells. Each point represents two independent determinations.

were separated on a 5 μm Supelcosil LC-8-DB column (4.6 mm × 25 cm; Supelco, Inc.). The mobile phase consisted of methanol/acetonitrile/1% formic acid in water (30:20:50, by vol.) which was pumped at a flow rate of 1 mL/min. The eluent was monitored at 269 nm, and the radioactivity was measured with a Berthold model LB 506C monitor (Berthold Analytical Instruments) fitted with a solid cell (YG400). Material obtained from bands A, B and C was designated Hep G2-derived crisnatol metabolites I, II and III, respectively. These metabolites correspond to two major bands at R_f values of 0.59 (I + II) and 0.66 (III) observed in cell medium on analytical plates (see Fig. 4A).

To the liver microsome incubation mixture, an equal volume of methanol/acetonitrile (1:1) was added and the mixture centrifuged at 3000 rpm for 10 min. The resultant supernatant was reduced to a small volume and then chromatographed on analytical silica gel TLC plates as described above. Autoradiograms of the developed plates revealed two major bands designated D (R_f 0.63) and E (R_f 0.80). The silica gel corresponding to each band was scraped off and the radioactivity eluted with methanol, which was then reduced to dryness. The residue was reconstituted in mobile phase and the metabolites were further purified by HPLC, as described above. The radiolabeled materials obtained from bands D and E were designated human liver-derived crisnatol metabolites IV and V, respectively. Metabolites IV and V correspond to the major bands observed at R_f values of 0.63 and 0.77, respectively, in Fig. 4C. The average HPLC retention times for metabolites II, III (or IV), and V, and crisnatol were 5.1, 5.9, 9.9, and 26.2 min, respectively.

GC/MS and NMR analysis. EI/MS of TMS derivatives of the crisnatol metabolites were obtained using a VG 70S double-focusing mass spectrometer (VG Analytical, Manchester, U.K.) after GC separation. TMS derivatives were formed by heating the metabolite sample with BSTFA/acetonitrile/dichloromethane (2:1:0.1, by vol.) at 100° for 30 min. GC was performed using a 10 m DB-5 capillary column (0.32 mm i.d., 25 μm thickness) (J&W, Folsom, CA) which was temperature programmed from 100 to 300° at 20°/min. The column was held

at 100° for 2 min after injection. The spectra were recorded at an ionization energy of 70 eV.

Proton NMR spectra were recorded in DMSO-d_6 solution at 25° on a Varian VXR-500S spectrometer operating at a frequency of 499.984 MHz.

RESULTS

Antiproliferative activity of crisnatol in Hep G2 cells. Antiproliferative activity of various concentrations of crisnatol in Hep G2 cells was assessed by measuring thymidine incorporation, cell growth, and vital staining of cells using neutral red dye.

Figure 1A illustrates a time- and concentration-dependent decrease in thymidine incorporation into acid-insoluble pools of Hep G2 cells cultured in the presence of crisnatol. Approximately 100% inhibition was achieved at crisnatol concentrations of 1.3 μg/mL within a 24-hr culture period. Crisnatol is very lipophilic and may disrupt cell membrane functions including transport processes. The crisnatol-mediated decrease in thymidine incorporation may have been caused artifactually by a decrease in intracellular soluble pools of thymidine resulting from an alteration in thymidine transport. This possibility was assessed by determining acid-soluble and acid-insoluble pools of thymidine in Hep G2 cells cultured in the presence of crisnatol for 48 hr. Crisnatol had no significant effect on [^{3}H]thymidine uptake or on intracellular soluble pools at concentrations of 1.3 μg/mL and lower. Hence, the crisnatol-mediated effect illustrated in Fig. 1A is not the result of alterations in intracellular radiolabeled pool sizes.

Consistent with these observations was the effect of crisnatol on the growth rate of Hep G2 cells. Figure 1B illustrates a concentration- and time-dependent decrease in cell number of Hep G2 cells cultured in the presence of crisnatol. The minimum concentration which produced no increase in cell number and approximately 0% thymidine incorporation was 1.3 μg/mL (Fig. 1, A and B). At this crisnatol concentration no overt cell lysis or other indications of acute cytotoxicity were observed microscopically.

Another measure of the antiproliferative effects of crisnatol was assessed using the vital stain, neutral red (which requires mitochondrial activity for activation). Figure 2 illustrates vital neutral red staining expressed as a percent of control cell values. It is interesting to note that Hep G2 cells incubated for 48 hr in the presence of 1.3 μg/mL crisnatol had 65% of the control dye staining yet thymidine incorporation was 0% of control and there was no cell growth. This suggests that 1.3 μg/mL crisnatol completely inhibits the replication of Hep G2 cells but cell viability is decreased by only 35%. These data were confirmed by Trypan blue exclusion in Hep G2 cells treated for 48 hr in the presence of 1.3 μg/mL crisnatol. Based on these data, metabolism studies using Hep G2 cells were performed at crisnatol concentrations of 0.05, 0.50 and 1.00 μg/mL medium.

[^{14}C]*Crisnatol metabolism by Hep G2 cells.* Hep G2 cells were incubated with [^{14}C]crisnatol (0.05, 0.50 and 1.00 μg/mL medium) at 37° for 24 hr. The

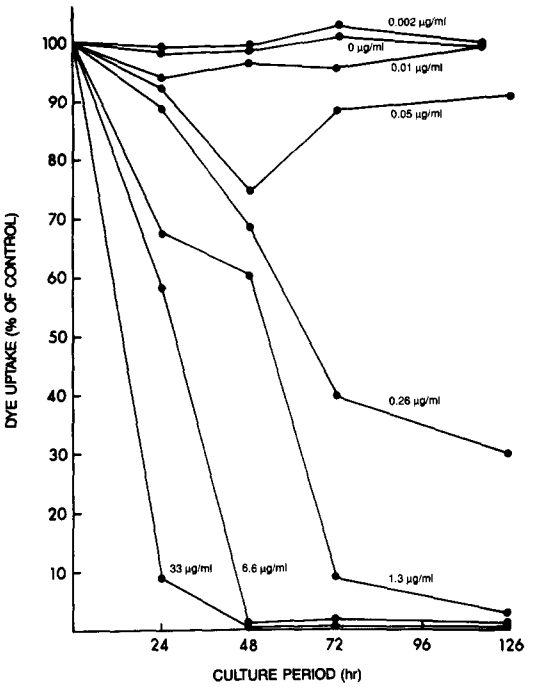

Fig. 2. Neutral red dye vital staining of Hep G2 cells cultured in the presence of various concentrations of crisnatol. Hep G2 cells were cultured in the presence of the indicated concentrations of crisnatol for 24, 48, 72 and 126 hr. The cells were stained with the vital stain, neutral red. Data are expressed as a percentage of controls, which received no treatment. O.D. values at 550 nm for the control samples at 24, 48, 72 and 126 hr were 0.53, 0.61, 0.82 and 0.93, respectively. The 0 μg/mL values represent vehicle-treated samples. Each point represents eight independent determinations.

majority (85.9%) of the radioactivity added to the culture was recovered in the cell medium and smaller amounts in the intracellular supernatant (6.2%), PBS rinse (2.4%), and cell debris (1.6%). TLC/autoradiographic analysis of the cell medium revealed several well-resolved drug-related radioactive bands, indicating extensive metabolism of crisnatol by Hep G2 cells (Fig. 3). Two major bands at R_f values of 0.59 and 0.66 accounted for 58% of the total radioactivity present in the medium (Fig. 4A). The other bands were present in smaller amounts ranging from 1.74 to 8.27% of the total radioactivity. After treatment of the cell medium with a β-glucuronidase/sulfatase mixture (in the absence and presence of saccharolactone, the inhibitor for β-glucuronidase), there was no significant change in the distribution of radioactivity associated with the bands between the control and the enzyme-treated samples, suggesting that glucuronide and/or sulfate conjugates were not present. The metabolite patterns of the material in the cell medium and intracellular supernatant were very similar but with quantitative differences (Fig. 4, A and B). The proportion of intact drug (R_f value of approximately 0.85) was lower in the cell medium (2.3%) compared to the intracellular supernatant (14.8%). A time course

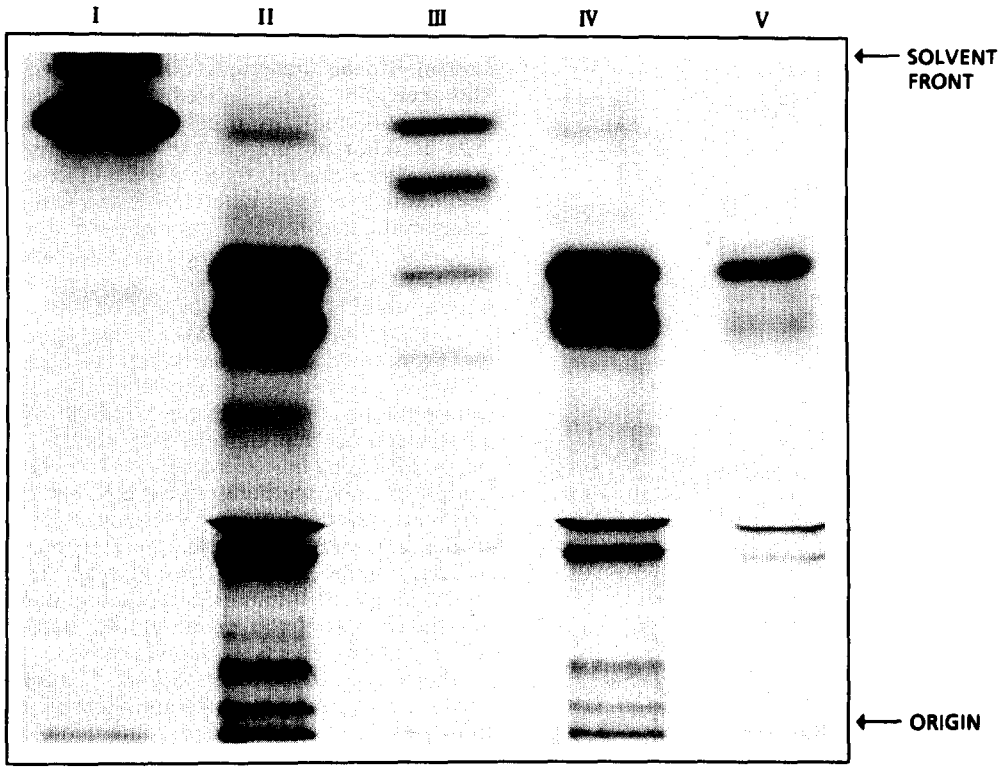

Fig. 3. Typical TLC/autoradiogram of crisnatol and metabolites in cell medium after incubation of [^{14}C]crisnatol with Hep G2 cells at 37° for 24 hr. Key: control sample (no cells, lane I); [^{14}C]crisnatol concentrations of 1.0 (lanes I and II), 0.5 (lane IV) and 0.05 μg/mL medium (lane V); metabolite profile in an extract of rat feces from an animal dosed orally with [^{14}C]crisnatol at 25 mg/kg (lane III).

study showed that after 5.5 hr approximately 60% of the total ^{14}C-labeled material recovered from the cell medium was intact drug, but by 24 hr it accounted for only 4% of the total radioactivity (data not shown).

[^{14}C]*Crisnatol metabolism by human liver microsomes.* There was extensive metabolism of [^{14}C]crisnatol by the human liver microsomes with the intact drug accounting for only about 8% of the radioactivity recovered from the mixture after a 24-hr incubation period (Fig. 4C). Major drug-related radioactive bands at R_f values of 0.33, 0.43, 0.51, 0.63, and 0.77 accounted for a mean of 8.5, 4.4, 6.0, 48.2, and 9.9%, respectively, of the radioactivity present in the incubation mixture.

Both Hep G2 cells and human liver microsomes form drug metabolites with chromatographic properties (TLC R_f) similar to metabolites observed in extracts of feces from rats dosed orally with [^{14}C]crisnatol (Fig. 3). The pattern of crisnatol metabolism observed in the two *in vitro* systems used in the present study does not appear to be concentration dependent, at least over the range used in this study.

Characterization of crisnatol metabolites produced by the Hep G2 cells and human liver microsomes. Hep G2-derived crisnatol metabolites I, II and III were well separated by GC, with I and II eluting before, and III after, crisnatol (TMS derivatives). The EI/MS of these three metabolites were almost identical. A typical mass spectrum obtained for metabolite III is shown in Fig. 5A. The observed parent ion, m/z 667, indicated the addition of 178 mass units to the TMS-derivative of crisnatol (m/z 489), consistent with the addition of two oxygen atoms, two hydrogen atoms, and two TMS groups to crisnatol. These data indicated that the three compounds are isomeric dihydrodiols. The ^{1}H-NMR spectrum of metabolite III was also consistent with the proposed dihydrodiol structure (Fig. 6A). The pair of doublets at 4.73 and 4.35 ppm were assigned to the 1- and 2-protons, respectively (Table 1). The 11 Hz coupling observed between these protons is indicative of a diaxial configuration, which is consistent with diequatorial *trans*-1,2 substitution of the hydroxyl groups. If the hydroxyl groups were at C-3,4 position, the corresponding protons would be expected to assume diequatorial orientation due to steric interactions in the "bay region," resulting in 2–4 Hz coupling between these protons. The EI/MS and NMR spectral data support metabolite III to be *trans*-1,2-dihydro-1,2-dihydroxycrisnatol (Fig. 7). Although GC/MS data indicate metabolites I and II to be isomeric dihydrodiol derivatives of crisnatol, they were not further characterized by NMR due to insufficient quantities available for analysis.

Crisnatol metabolites IV and V isolated from human liver microsomes correspond to the two

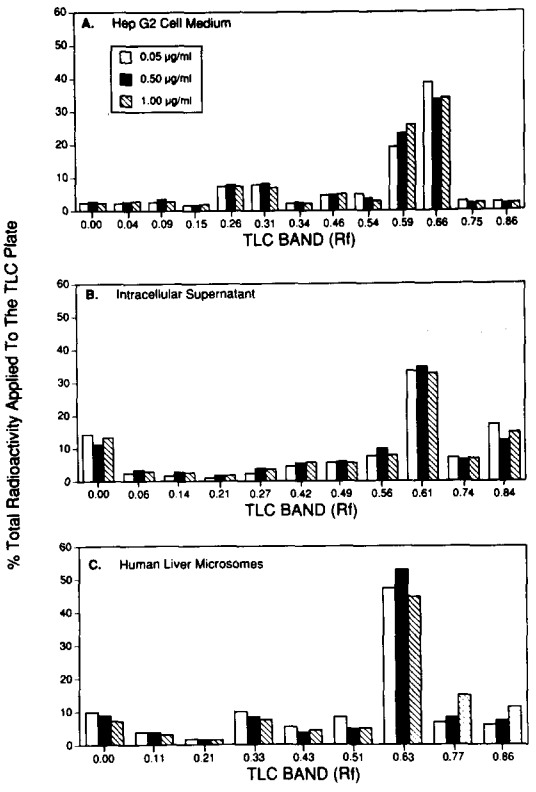

Fig. 4. TLC profile of crisnatol and metabolites in Hep G2 cell medium (A), intracellular supernatant (B) and human liver microsomes (C) after incubation of [^{14}C]crisnatol at 37° for 24 hr. Crisnatol R_f value was 0.86.

major bands observed at R_f 0.63 (D) and 0.77 (E), respectively, in Fig. 4C. GC/MS analysis of the material isolated from band D indicated the presence of two peaks with the larger component (approximately 90% of the total), metabolite IV, eluting after crisnatol on the GC column. Their EI/MS were similar and were indistinguishable from the isomeric dihydrodiol derivatives of crisnatol formed by the Hep G2 cell. The proton NMR spectrum for metabolite IV was very similar to that of metabolite III (Fig. 6, B and A, respectively), clearly establishing the structure of IV, also as the *trans*-1,2-dihydro-1,2-dihydroxycrisnatol (Fig. 7). The EI/MS of metabolite V (Fig. 5B) gave a molecular ion at m/z 577 indicative of the addition of 88 mass units to the TMS-derivative of crisnatol (m/z 489). This is consistent with the monohydroxylation of the chrysene ring in the parent compound. The large peak at m/z 329 corresponds to the loss of the side chain at the methylamino-bond. Additional characteristic ions at m/z 474 and 562 were due to the loss of CH_2OTMS and CH_3 groups, respectively, from the parent ion. The ^{1}H-NMR spectrum of metabolite V (Fig. 6C) indicated that hydroxylation occurred at the C-1 position on the chrysene ring (Fig. 7).

DISCUSSION

A number of recent reports (see introduction) suggest that the human hepatoma cell line Hep G2 may be a useful *in vitro* model system for studying human hepatic drug metabolism. However, since this cell line was derived from tumor cells (hepatoblastoma), its drug-metabolizing activities may be different compared to normal human liver tissue. Since the metabolic profile of crisnatol in humans has yet to be determined, as a first step we compared and contrasted the metabolic capacity of Hep G2 cells and human liver microsomes. In addition, we also investigated the antiproliferative properties of crisnatol on Hep G2 cells.

Crisnatol metabolism studies using Hep G2 cells were conducted at three concentrations ranging from minimal to maximum antiproliferative effective concentrations. The acute antiproliferative effects of crisnatol on Hep G2 cells were similar to those reported in other *in vitro* systems [4, 32]. The precise antiproliferative mechanism(s) of action of crisnatol still remains to be elucidated. At present it is unclear if this antiproliferative effect results from direct cellular interactions with crisnatol and/or active metabolite(s). It is important to note that even the maximal antiproliferative concentration had minimal acute cytotoxic effects in Hep G2 cells.

There was extensive metabolism of crisnatol by Hep G2 cells and human liver microsomes. Hep G2 cells produced three isomeric dihydrodiols as the major metabolites of crisnatol (a chrysene based compound) and one of these, metabolite III (the major isomer), was identified by GC/MS and ^{1}H-NMR as *trans*-1,2-dihydro-1,2-dihydroxycrisnatol (Fig. 7). The other two dihydrodiols could not be further characterized by NMR due to insufficient quantities of material available for analysis. Our data on dihydrodiol formation are consistent with the earlier findings that the metabolism of benzo[*a*]pyrene (BP) by Hep G2 cells also results in the formation of isomeric dihydrodiols and, in addition, phenol derivatives of BP [21]. Biotransformation of crisnatol by Hep G2 cells also led to the formation of minor amounts of at least seven other products (see Fig. 3, lane II). The TLC chromatographic behavior (R_f value) of some of these metabolites represented by ^{14}C-bands was similar to the metabolites isolated from feces of rats dosed orally with [^{14}C]crisnatol (Fig. 3, see lanes II and III). Biotransformation of crisnatol by the rat mainly involves hydroxylation and dihydrodiol formation in the chrysene ring, and oxidation of the propanediol side chain resulting in the formation of three major fecal metabolites [6, 33].

Formation of monohydroxy and dihydrodiol metabolites for crisnatol was to be expected based upon work that explored the metabolism of the unsubstituted chrysene molecule by rat liver microsomes [34]. In that work three *trans*-dihydrodiols (chrysene 1,2-diol, 3,4-diol and 5,6-diol) were formed and accounted for 65–76% of the total metabolites. The 1,2- and 3,4-dihydrodiols were the major metabolites. Further activation products of chrysene dihydrodiols, including the diol-epoxides, phenolic-diols, and tetrols have also been reported [35–37]. In the current work, although minor metabolites of crisnatol were formed, they have not been identified. It is reasonable to speculate based

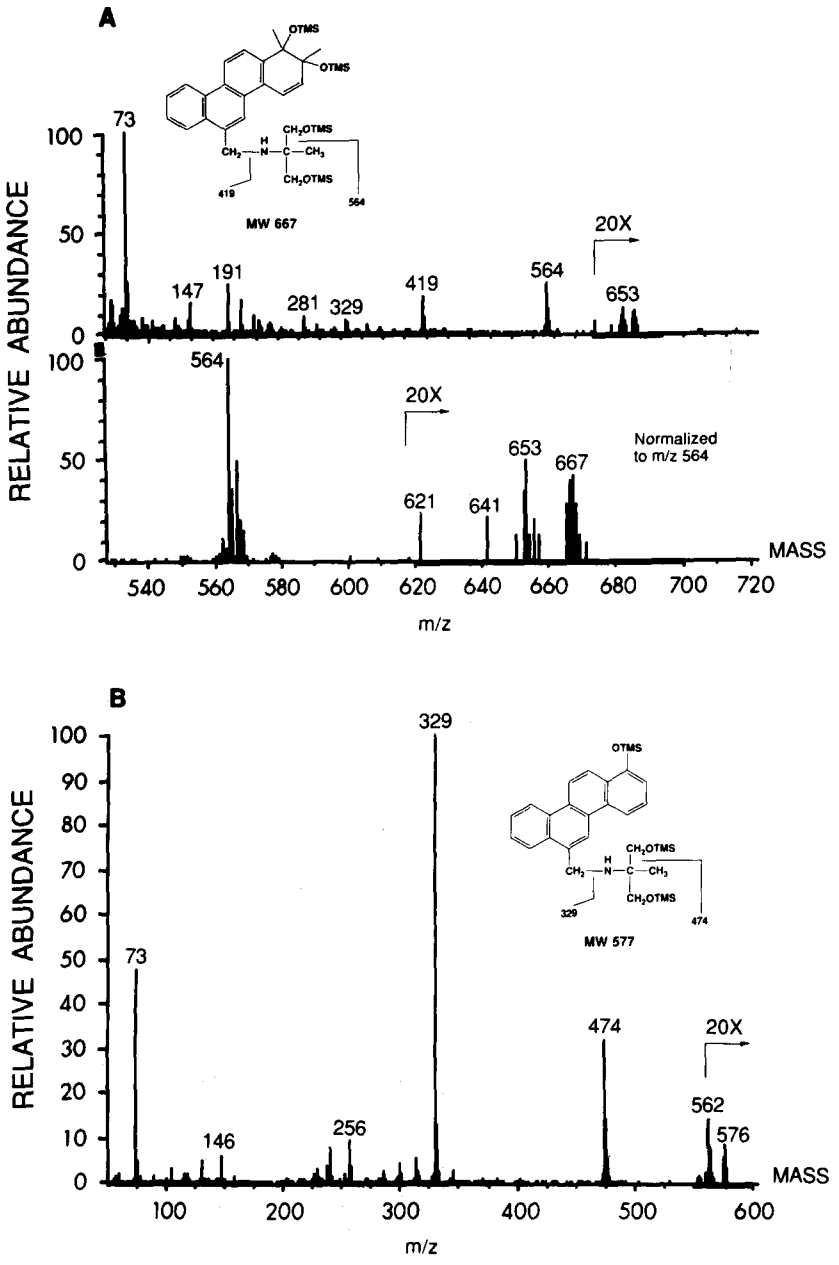

Fig. 5. EI/MS (TMS derivatives) of crisnatol metabolite III isolated from Hep G2 cells (A) and metabolite V isolated from human liver microsomes (B).

upon the rat microsomal work that the two minor isomeric crisnatol dihydrodiols formed by Hep G2 cells are the 3,4- (or 9,10-) and 7,8-dihydrodiol isomers. Incubation of crisnatol with human liver microsomes also produced two isomeric dihydrodiols with 1,2-dihydrodiol as the major isomer (accounting for 90% of the mixture) and, in addition, 1-hydroxycrisnatol (Fig. 7).

Epoxides have been identified as common intermediates in the metabolic formation of phenols and dihydrodiols [38]. Thus, the formation of phenols via spontaneous isomerization of epoxides and the enzymatic hydration of the same epoxides resulting in the formation of dihydrodiols are both competing pathways in the metabolism of polycyclic aromatic hydrocarbons in mammals. The activity of epoxide hydrolase, an enzyme which catalyzes the hydration of epoxides to *trans*-dihydrodiols, has been reported to be about 6-fold higher in the Hep G2 cells compared with normal human hepatocytes [19]. This is consistent with our findings of isomeric dihydrodiols, and not phenols as the major metabolites of crisnatol formed by the Hep G2 cells. In the present study we were unable to show the

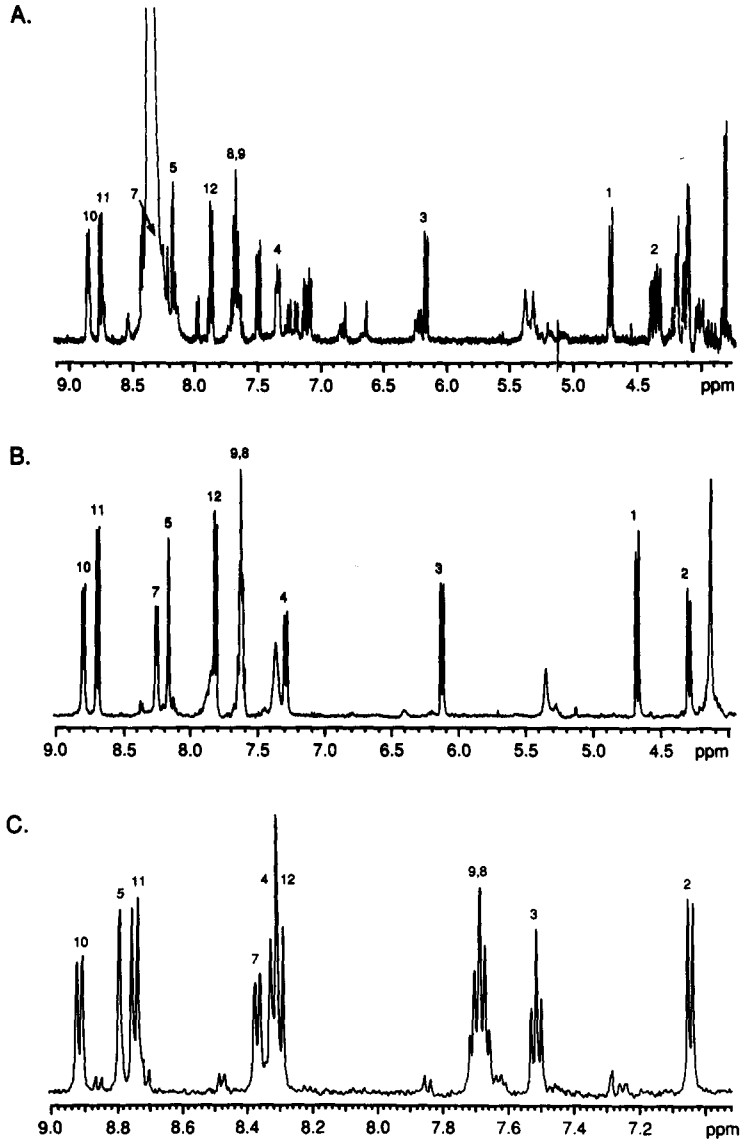

Fig. 6. ^{1}H-NMR spectra of the aromatic region of crisnatol metabolite III isolated from Hep G2 cells (A), and metabolites IV (B) and V (C) isolated from human liver microsomes using DMSO-d_6 as the solvent.

Table 1. ^{1}H-NMR Spectral data for crisnatol and metabolites

	Aromatic protons and chemical shifts (ppm) in DMSO-d_6										
Compound	H1	H2	H3	H4	H5	H7	H8	H9	H10	H11	H12
Crisnatol	8.16	7.82	7.76	8.95	9.12	8.42	7.84	7.85	9.07	8.94	8.20
Metabolite III	4.73	4.35	6.24	7.36	8.17	8.30	7.75	7.75	8.92	8.79	7.94
Metabolite IV	4.70	4.32	6.15	7.31	8.18	8.27	7.64	7.64	8.80	8.70	7.83
Metabolite V		7.08	7.55	8.35	8.82	8.40	7.72	7.72	8.94	8.77	8.33

Coupling constants for metabolite IV (Hz): $J_{1,2} = 11.2$; $J_{2,3} = 1.9$; $J_{3,4} = 9.8$; $J_{7,8} = 8.3$; $J_{9,10} = 8.5$; $J_{11,12} = 8.5$.

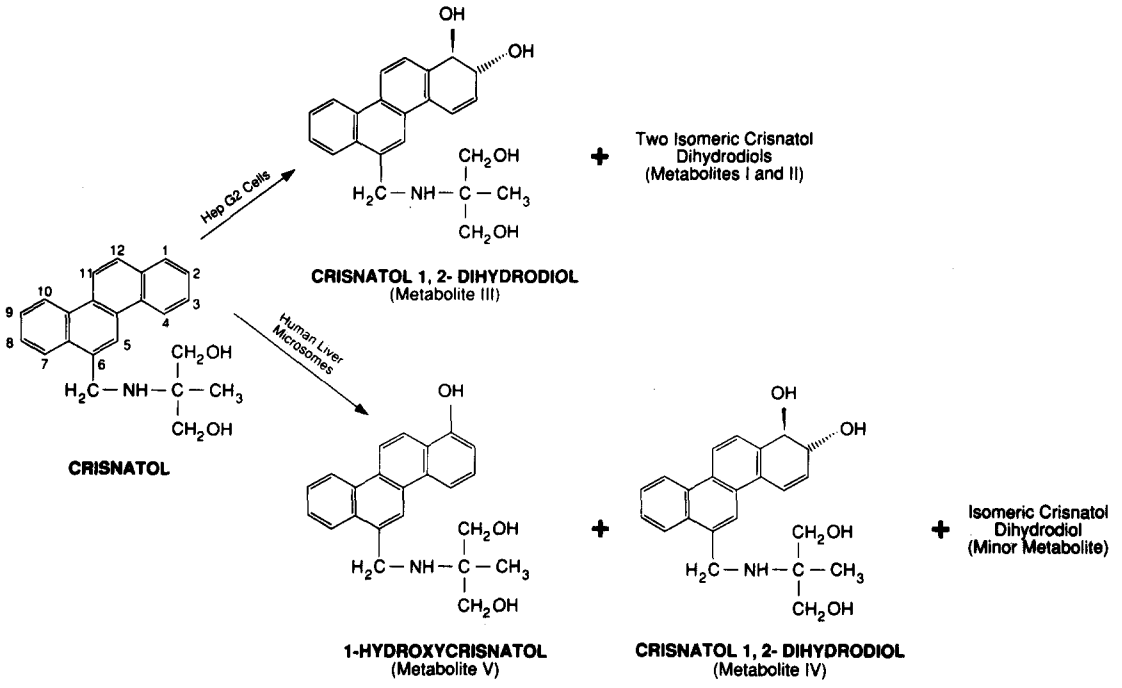

Fig. 7. Chemical structures of crisnatol and metabolites.

presence of glucuronic acid and sulfate conjugates of crisnatol or metabolites in medium from Hep G2 cells incubated with crisnatol probably due to the low levels of UDP-glucuronyltransferase and sulfotransferase activities reported in this cell line [16, 19] and also because of the lack of formation of significant quantities of the phenol metabolite(s) of crisnatol, which are more suitable substrates for these conjugation reactions than dihydrodiols.

Hep G2 cells offer certain advantages as a system for studying human liver drug metabolism compared to other *in vitro* systems such as liver microsomes: (1) Hep G2 cells are easily available and may provide an unlimited source of reproducible material, (2) whole cells preserve much of the cellular complexity which is lost during subcellular fractionation and therefore more closely resemble the *in vivo* physiological environment, and (3) variability in drug-metabolizing enzyme activities due to individual liver preparations is minimized with Hep G2 cells which are intrinsically more reproducible. Additional research remains to be done to further characterize the nature of the drug-metabolizing capacity (both the phase I and II reactions) of Hep G2 cells not yet determined, and how these activation and detoxification reactions compare with the *in vivo* profile in humans and with those in other *in vitro* systems using normal human liver tissue (e.g. hepatocytes, liver slices, and microsomes).

In conclusion, it is clear from the present study that a derivative of chrysene, crisnatol, is metabolized in a way similar to the unsubstituted chrysene by the human liver-derived cell line, Hep G2, and human liver microsomes. Isomeric dihydrodiols were the major metabolites formed by both systems and, in addition, a monohydroxy compound was also produced by human liver microsomes. Hep G2 cells also formed a number of other metabolites which had chromatographic properties (TLC R_f value) similar to crisnatol metabolites formed by the rat, including the 1-hydroxycrisnatol (R_f 0.74 to 0.75). Thus, the formation of the 1-hydroxy derivative of crisnatol by Hep G2 cells cannot be ruled out. Since, the rat also forms these crisnatol metabolites, it is likely that the dihydrodiol and monohydroxy derivatives of crisnatol will be formed by humans.

Acknowledgement—The authors wish to thank Andrea Resetar for providing the human liver microsomes.

REFERENCES

1. Bair KW, Tuttle RL, Knick VC, Cory M and McKee DD, (1-Pyrenylmethyl)aminoalcohols, a new class of antitumor DNA intercalators. Discovery and initial amine side chain structure–activity studies. *J Med Chem* **33**: 2385–2393, 1990.
2. Knick VC, Tuttle RL, Bair KW and Von Hoff DD, Murine and human tumor stem cell activity of three candidate arylmethylaminopropanediols (AMAP). *Proc Am Assoc Cancer Res* **27**: 424, 1986.
3. Adams DJ, Tuttle RL, Knick VC and Wilson JG, Characterization of *in vivo* resistance to BW A770U, a novel arylmethylaminopropanediol (AMAP) antitumor agent. *Proc Am Assoc Cancer Res* **27**: 424, 1986.
4. Adams DJ, *In vitro* pharmacodynamic assay for cancer drug development: Application to crisnatol, a new DNA intercalator. *Cancer Res* **49**: 6615–6620, 1989.
5. Woolley JL Jr, Wargin WA, Hsieh A, Liao SHT, Blum MR, Crouch RC and Sigel CW, Disposition of

arylmethylaminopropanediol, BW-A770U, in the rat and dog. *Proc Am Assoc Cancer Res* **27**: 423, 1986.
6. Patel DK, Sigel CW, Shockcor JP and Taylor LCE, Metabolism and disposition of the arylmethylaminopropanediol (AMAP) BW A770U in the rat after oral dose. *Proc Am Assoc Cancer Res* **28**: 442, 1987.
7. Patel DK, Wargin WA and Sigel CW, Disposition and metabolism of the novel antitumor agent crisnatol (BW A770U) in the male beagle dog. *Proc Am Assoc Cancer Res* **30**: 535, 1989.
8. Harman GS, Craig JB, Kuhn JG, Luther JS, Turner JN, Weiss GR, Tweedy DA, Koeller J, Tuttle RL, Lucas VS, Wargin W, Whisnant JK and Von Hoff DD, Phase I and clinical pharmacology trial of crisnatol (BWA 770U mesylate) using a monthly single-dose schedule. *Cancer Res* **48**: 4706–4710, 1988.
9. Aden DP, Fogel A, Plotkin S, Damjanov I and Knowles BB, Controlled synthesis of HBsAg in a differentiated human liver carcinoma-derived cell line. *Nature* **282**: 615–616, 1979.
10. Schwartz AL and Rup D, Biosynthesis of the human asialoglycoprotein receptor. *J Biol Chem* **258**: 11249–11255, 1983.
11. Schwartz AL, Fredovich SE, Knowles BB and Lodish HF, Characterization of the asialglycoprotein receptor in a continuous hepatoma line. *J Biol Chem* **256**: 8878–8881, 1981.
12. Huber BE, Glowinski IB and Thorgeirsson SS, Transcriptional and post-transcriptional asialglycoprotein receptor in normal and neoplastic liver. *J Biol Chem* **261**: 12400–12407, 1986.
13. Knowles BB, Howe CC and Aden DP, Human hepatocellular carcinoma cell lines secrete the major plasma proteins and hepatitis B surface antigen. *Science* **209**: 497–499, 1980.
14. Moses AC, Freinkel AJ, Knowles BB and Aden DP, Demonstration that a human hepatoma cell line produces a specific insulin-like growth factor carrier protein. *J Clin Endocrinol Metab* **56**: 1003–1008, 1983.
15. Zannis VI, Breslow JL, Aden DP, San Giacomo TR and Knowles BB, Characterization of the major apolipoproteins secreted by two human hepatoma cell lines. *Biochemistry* **20**: 7089–7096, 1981.
16. Dawson JR, Adams DJ and Wolf CR, Induction of drug metabolizing enzymes in human liver cell line Hep G2. *FEBS Lett* **183**: 219–222, 1985.
17. Sassa S, Sugita O, Galbraith RA and Kappas A, Drug metabolism by the human hepatoma cell, Hep G2. *Biochem Biophys Res Commun* **143**: 52–57, 1987.
18. Duthie SJ, Coleman CS and Grant MH, Status of reduced glutathione in the human hepatoma cell line, Hep G2. *Biochem Pharmacol* **37**: 3365–3368, 1988.
19. Grant MH, Duthie SJ, Gray AG and Burke MD, Mixed-function oxidase and UDP-glucuronyltransferase activities in the human Hep G2 hepatoma cell line. *Biochem Pharmacol* **37**: 4111–4116, 1988.
20. Dearfield KL, Jacobson-Kram D, Brown NA and Williams JR, Evaluation of a human hepatoma cell line as a target cell in genetic toxicology. *Mutat Res* **108**: 437–449, 1983.
21. Abe S, Nemoto N and Sasaki M, Sister-chromatid exchange induction by direct mutagens/carcinogens, arylhydrocarbon hydroxylase activity and benzo-[*a*]pyrene metabolism in cultured human hepatoma cells. *Mutat Res* **109**: 83–90, 1983.
22. Huh N, Nemoto N and Utakoji T, Metabolic activation of benzo[*a*]pyrene, aflatoxin B_1, and dimethylnitrosamine by a human hepatoma cell line. *Mutat Res* **94**: 339–348, 1982.
23. Diamond L, Kruszewski F, Aden DP, Knowles BB and Baird WM, Metabolic activation of benzo[*a*]pyrene by a human hepatoma cell line. *Carcinogenisis* **1**: 871–875, 1980.
24. Buenaventura SK, Jacobson-Kram D, Dearfield KL and Williams JR, Induction of sister chromatid exchange by diethylstilboesterol in metabolically competent hepatoma cell lines but not in fibroblasts. *Cancer Res* **44**: 3851–3855, 1984.
25. Ranganathan S and Kottke BA, Studies on the regulation of cholesterol metabolism by low- and high-density lipoproteins in Hep G2 cells. *Hepatology* **9**: 547–551, 1989.
26. Tam S-P, Strugnell S, Deeley RG and Jones G, 25-Hydroxylation of vitamin D_3 in the human hepatoma cell lines Hep G2 and Hep 3B. *J Lipid Res* **29**: 1637–1642, 1988.
27. Chu AJ, Secretion of metabolites of 5 alpha-cholest-8(14)-en-3 beta-ol-15-one by Hep G2 cells. *Proc Natl Sci Counc Repub China* **12**: 209–214, 1988.
28. Huber BE and Thorgeirsson SS, Analysis of c-*myc* expression in a human hepatoma cell line. *Cancer Res* **47**: 3414–3420, 1987.
29. Huber BE and Brown NA, 12-*O*-Tetradecanoylphorbol-13-acetate actions on macromolecular synthesis, ornithine decarboxylase, and cellular differentiation of the rat embryonic visceral yolk sac in culture. *Cancer Res* **43**: 5552–5559, 1983.
30. Huber BE and Cordingley MG, Expression and phenotypic alterations caused by an inducible transforming *ras* oncogene introduced into rat liver epithelial cells. *Oncogene* **3**: 245–256, 1988.
31. Resetar A and Spector T, Glucuronidation of 3′-azido-3′deoxythymidine: Human and rat enzyme specificity. *Biochem Pharmacol* **38**: 1389–1393, 1989.
32. Bellamy W, Dorr R, Bair K and Alberts D, Cytotoxicity and mechanism of action of 3-arylmethylaminopropanediols (AMAPS). *Proc Am Assoc Cancer Res* **30**: 562, 1989.
33. Patel DK, Woolley JL Jr, Shockcor JP, Johnson RL and Sigel CW, Disposition, metabolism and excretion of the anticancer agent crisnatol in the rat. *Drug Metab Dispos* **19**: 491–497, 1991.
34. Nordqvist M, Thakker DR, Vyas KP, Yagi H, Levin W, Ryan DE, Thomas PE, Conney AH and Jerina DM, Metabolism of chrysene and phenanthrene to bay-region diol epoxides by rat liver enzymes. *Mol Pharmacol* **19**: 168–178, 1981.
35. Grover PL, Pathways involved in the metabolism and activation of polycyclic hydrocarbons. *Xenobiotica* **16**: 915–931, 1986.
36. Glatt H, Seidel A, Bochnitschek W, Marquardt H, Hodgson RM, Grover PL and Oesch F, Mutagenic and cell-transforming activities of trio-epoxides as compared to other chrysene metabolites. *Cancer Res* **46**: 4556–4565, 1986.
37. Weems HB, Fu PP and Yang SK, Stereoselective metabolism of chrysene by rat liver microsomes. Direct separation of diol enantiomers by chiral stationary phase HPLC. *Carcinogenesis* **7**: 1221–1230, 1986.
38. Jerina DM and Daly JW, Arene oxides: A new aspect of drug metabolism. *Science* **185**: 573–582, 1974.